Available online at www.sciencedirect.com
SCIENCE DIRECT®
Polymer 45 (2004) 2433–2442
polymer
www.elsevier.com/locate/polymer

Micromechanical modeling of elastic properties in polyolefins

F. Bédoui[a], J. Diani[a], G. Régnier[b,*]

[a]Laboratoire de Microstructure et Mécanique des Matériaux (LM3-CNRS UMR 8006) ENSAM, 151 bd de l'Hôpital 75013, Paris, France
[b]Department of Materials, Laboratoire de Transformation et Vieillissement des Polymères (LTVP) ENSAM, 151 bd de l'Hôpital 75013, Paris, France

Received 31 October 2003; received in revised form 19 January 2004; accepted 19 January 2004

Abstract

The aim of this article is to try to explain why isotactic polypropylene (PP) is stiffer than high density polyethylene (HDPE) despite the fact that this latter is more crystalline and that its crystallites are stiffer than PP ones. Two micromechanical models were chosen for their ability to represent semi-crystalline polymers. The first one is a differential scheme in which ellipsoidal crystallites are randomly dispersed in an amorphous matrix. The second one is a self-consistent scheme where the material is considered as an aggregate of randomly oriented two layered-phase composite inclusions (crystalline–amorphous). Experiment-model comparisons are clearly in favor of the first model. This latter demonstrates the key importance of the crystalline lamellae aspect ratio on the elastic properties of semi-crystalline polymers.

Keywords: Micromechanical modeling; Semi-crystalline polymers; Elasticity

1. Introduction

Nowadays, thermoplastic materials are increasingly used in industrial parts. It is especially true for semi-crystalline materials, which are widely used as structural materials. During the part forming, the stretching or the shearing of the polymer melt under strong cooling conditions lead to a flow-induced crystallization, which generates specific crystalline morphologies such as deformed spherulites, shish–kebab or more complex crystalline macrostructure like in polypropylene for example [1]. A high anisotropy of molecular orientation in the crystalline phase is resulting [2,3], even for solidifying shear flows [4–6]. Moreover crystallinity variations along the part and in the part depth can be observed [7]. The crystalline orientation is responsible for possible anisotropic behavior, while variations of the amount of crystallinity induce strong variations of the mechanical properties [8].

For structural polymer applications, there is an industrial need for the prediction of these mechanical properties, especially for the small-deformation behavior, to determine for example the strength of blown bottles [9] or the shrinkage and the warpage of injected parts [10]. Now, process simulations including a flow-induced crystallization law coupled to a viscoelastic behavior based on molecular models [11], allow to predict the final crystallinity and the final molecular orientation in the crystalline phase [12,13]. But, from the predicted crystalline morphology of the polymer, little was done to predict the mechanical properties. Although micromechanical modeling is efficiently used to determine the thermomechanical properties of filled polymers [14], only a few researchers applied these micro–macro models to non-filled semi-crystalline polymers.

Halpin and Kardos [15] proposed to use Halpin–Tsai model [16] in order to determine the elastic moduli of semi-crystalline polymers. The model requires the assumption that lamellae be regarded as fibers. Phillips and Patel [17] applied this model to PE. An adjustable parameter in this model was linked to crystallite shape ratio. However, this model, which is generally used to calculate the moduli of short-fiber composite, is known to fit only the experimental data at low volume fraction of filler. This is not the case of semi-crystalline materials, for which the crystallinity can often reach 60–70%.

Later, several researchers worked on the prediction of the large deformation behavior to predict the texture evolution induced by a plastic deformation [18,19]. Lee et al. [18] developed a specific micromechanical model in which the crystalline lamellae were assumed to be rigid-visco-plastic and the amorphous phase visco-plastic. Nikolov and Doghri

* Corresponding author. Tel.: +33-1-44246305; fax: +33-1-44246382.
E-mail address: gilles.regnier@paris.ensam.fr (G. Régnier).

0032-3861/$ - see front matter © 2004 Elsevier Ltd. All rights reserved.
doi:10.1016/j.polymer.2004.01.028

Table 1
Some physical and mechanical properties of PP *ELTEX HV 252* and PE *HD6070 EA*

Polymer	MFI (g/10 min) (2.16 kg 230 °C)	M_n (kg/mol)	M_w (kg/mol)	Young's modulus (MPa)	Poisson's ratio	Mean volume crystallinity (%)
HDPE	7	12	70	1200	0.46	70
PP	11	25	180	1400	0.42	57

[20] adapted the previous model in a Sachs-inclusion model for the small-deformation behavior by assuming a visco-elastic behavior for the amorphous phase. This modeling, which leads to a lower bound for the micromechanics modeling, should underestimate the experimental moduli. More recently, van Dommenlen et al. [21] have also adapted the Lee et al.'s model [18] by assuming the behavior of the amorphous phase as isotropic elastic with plastic flow being a rate-dependent process with strain hardening resulting from molecular orientation and the one of the crystalline phase as anisotropic elastic with plastic flow occurring via crystallographic slip. The behavior of polymer is simulated until large deformation scale. The elasto-plastic-stress–strain behavior of HDPE during monotonic and cyclic loadings and the evolution of morphology were studied. Their results agree globally well with literature values, but the predicted initial moduli variation of PE versus the crystalline fraction does not fit the experimental values. No shape factors, which could describe the crystallite geometry, are introduced in the recent works.

The aim of this paper is to show how micromechanical modeling can predict the elastic behavior of polypropylene and polyethylene. Of course, even for small deformations, it is well known that these polymers have a visco-elastic behavior, even a visco-elasto-plastic behavior, but let us first evaluate the relevance of micromechanical modeling on the prediction of elastic properties of two different isotropic polymers at ambient temperature.

2. Micromechanical modeling

At a microscopic scale, semi-crystalline polymers are heterogeneous materials consisting of co-existing amorphous and crystalline phases. The crystalline phase consists mainly of crystal lamellae. In a relaxed polymer melt, the principal crystal lamellae grow radially from nucleation sites into a spherulitic texture, therefore the polymer chains are oriented perpendicular to spherulite radii. The lamellae are not always isolated entities, but joined together by branch-points, especially in polypropylene [1]. Moreover, the stress in the polymer is transmitted between the two phases through tie-molecules and that content of tie-molecules depends on crystallization conditions. Nevertheless, crystallite lamellae will be considered in our work as embedded into the amorphous phase, assuming that crystalline branch-points are weak links and that tie-molecules do not play a role in the small deformation scale.

Here, heterogeneities are considered at the sub-spherulitic scale and the two constitutive phases are the crystal lamellae and the amorphous phase. To investigate on the ability of micromechanics modeling to predict the homogeneous elastic behavior of semi-crystalline polymers, two materials are considered, polypropylene and polyethylene. Micromechanical modeling requires parameters such as behavior type, volume fraction and morphology of each constitutive phase. All these parameters are now discussed.

2.1. Material description

Two commercial homopolymers were supplied by Solvay: polypropylene PP ELTEX HV 252 and high density polyethylene (HDPE) PE HD6070 EA. The average molecular weight and the polydispersity index were determined by Solvay by means of gel permeation chromatography. The Young's modulus and the Poisson's ratio were measured at ambient temperature on 4 mm thick injection-molded samples by tensile tests on an Instron 4502 machine equipped with a mechanical Instron bi-axial extensometer. The test conditions were set according to the standard ISO 527. The mean crystallinity was determined from density measurement considering a single crystalline phase in each polymer: α phase for PP and the orthorhombic phase for HDPE. Physical and mechanical properties for both materials are given in Table 1. The Young's modulus of other quoted PE versus density or crystallinity is extracted from BP-Solvay Polyethylene database.

2.1.1. Characterization of the amorphous phase

For both polymers under study, the glass transition temperature of the amorphous phase is lower than ambient temperature; therefore the amorphous phase is in the rubbery state at ambient temperature. Chain entanglements are the cause of rubber-elastic properties in the liquid state and the kinetic theory of rubber elasticity, which was particularly developed by Flory [22], leads to the following equation for the amorphous phase of thermoplastic polymers above the glass transition temperature [23]:

$$G_N^0 = \frac{\rho RT}{M_e} \tag{1}$$

where G_N^0 is the shear modulus at plateau, ρ the amorphous phase density, R the ideal gas constant, T the temperature and M_e the molar mass between entanglements. The modulus at plateau G_N^0, which can be determined by

rheological measurements, is independent of chain length and not much sensitive to temperature. The molar mass between entanglements M_e is a material property, which can be considered temperature independent. M_e values (Table 2) are deduced from rheological measurements at high temperature [23–25]. Nevertheless, as both polymers cannot be obtained in a fully amorphous state at ambient temperature, G_N^0 values have to be extrapolated through Eq. (1). M_e is chosen equal to 7 kg/mol for PP and to 1.4 kg/mol for PE (Table 2), the amorphous phase density at ambient temperature is taken equal to 850 kg/m^3 for PP and 855 kg/m^3 for PE [26], then G_N^0 at ambient temperature is equal to 1.5 MPa for PE and 0.3 MPa for PP (Eq. (1)). Hence the Young's modulus of the amorphous phase at ambient temperature, which is equal to three times the shear modulus, was found equal to $E_{PE}^{am} = 4.5$ MPa for PE and $E_{PP}^{am} = 0.9$ MPa for PP.

Since the amorphous phase of the studied polymers is in the rubbery state, its Poisson's ratio is very close to 0.5, but slightly lower. To get coherent elastic properties, the Poisson's ratio ν is calculated using the classical relation [26]:

$$B = \frac{E}{3(1-2\nu)} \tag{2}$$

where the bulk modulus B is extrapolated at ambient temperature from PVT data [27] thanks to its definition relation:

$$\frac{1}{B} = \frac{1}{V}\frac{\partial V}{\partial p} \tag{3}$$

V being the specific volume. The determined values of bulk modulus ($B_{PP}^{am} = 2200$ MPa and $B_{PE}^{am} = 3000$ MPa) are close to the literature ones [26].

2.1.2. Crystalline phase characterization

The crystalline phase consists of polymer lamellae, which show a highly anisotropic behavior with a very high modulus along the chain axis. Elastic constants have been theoretically calculated for several materials and are reviewed by Ward [2]. For PE, the theoretical values of the stiffness tensor seem to largely overestimate the measured ones [28]. The polymer crystal stiffness is related to the conformation of the molecular chain [29]. The polyethylene chain has a planar-zigzag conformation, which justifies a theoretical modulus as high as 300 MPa along the chain direction. However, dynamical calculations have demonstrated the high dependence of the modulus on the chain contraction and when the chain contracts slightly from the planar-zigzag conformation, the modulus along the chain axis drops drastically. Tashiro et al. [29] suggest that, as the α-form nylon-6, the PE polymer chain experiences a thermal motion at room temperature and contracts from the planar-zigzag conformation, which induces a drop in modulus. Experimental measurements on ultra drawn HDPE have strengthened the idea that the value of theoretical modulus in the chain axis cannot be reached [28]. Therefore the moderate elastic stiffness tensor at ambient temperature could be, as proposed by Choy and Leung [28]:

$$\mathbf{C}_{PE}^{c} = \begin{pmatrix} 7.0 & 3.8 & 4.7 & 0 & 0 & 0 \\ 3.8 & 7.0 & 3.8 & 0 & 0 & 0 \\ 4.7 & 3.8 & 81 & 0 & 0 & 0 \\ 0 & 0 & 0 & 1.6 & 0 & 0 \\ 0 & 0 & 0 & 0 & 1.6 & 0 \\ 0 & 0 & 0 & 0 & 0 & 1.6 \end{pmatrix} \text{GPa} \tag{4}$$

where direction 3 refers to the chain axis, direction 1 to the lamella growth and direction 2 is represented in a manner as (e_1, e_2, e_3) defines a direct frame. This elasticity tensor seems especially appropriate for micromechanical calculations. van Dommelen et al. [21] have recently used this same tensor for their micromechanical modeling of elasto-viscoplastic behavior of polyethylene.

For polypropylene, the molecular chain has a helical conformation angle which is less dependent on the temperature [29]; hence the theoretical stiffness tensor as calculated by Tashiro et al. [30] would be:

$$\mathbf{C}_{PP}^{c} = \times \begin{pmatrix} 7.78 & 3.91 & 3.72 & 0 & 0.9 & 0 \\ 3.91 & 11.55 & 3.99 & 0 & -0.36 & 0 \\ 3.72 & 3.99 & 42.44 & 0 & -0.57 & 0 \\ 0 & 0 & 0 & 4.02 & 0 & -0.12 \\ 0.9 & -0.36 & -0.57 & 0 & 3.1 & 0 \\ 0 & 0 & 0 & -0.12 & 0 & 2.99 \end{pmatrix} \text{GPa} \tag{5}$$

This theoretical tensor agrees with the X-ray observed value of 40 GPa along the chain direction [31].

2.1.3. Morphology

At this step, let us note an interesting paradox: in spite of

Table 2
Rheological measurement of moduli at plateau and calculated molar masses between entanglements for PE and PP

Polymer	T (K)	ρ (kg/m^3)	Measured G_N^0 (Mpa)	M_e (kg/mol)
PE [23]	463	760	2.06	1.42
PE [24]	463	769	2.1	1.39
iPP [25]	463	765	0.42	7.02
aPP [25]	463	766	0.43	6.86

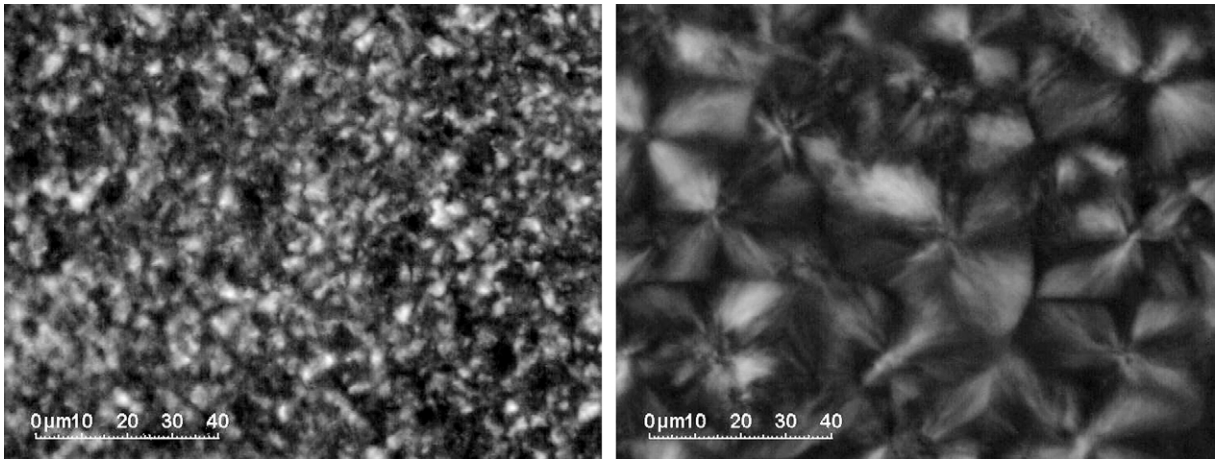

Fig. 1. Spherulitic morphology in the core of injected samples: PE on the left and PP on the right.

a much higher volume fraction of crystalline phase, a much higher crystalline modulus along the chain direction and an elastic modulus of the amorphous phase of the same order, the Young's modulus of HDPE is lower than the PP one, both polymers being in a macroscopically isotropic state. This paradox has to be explained by consideration of a morphological parameter.

The lamella thickness can be measured by small angle X-ray scattering (SAXS). The comparison of the crystalline layer thicknesses of several polymers [32] has shown that PE lamellae are thicker than PP ones. In this work, the PP lamellae thickness is about 10 nm while the lamella thickness for HDPE is closer to 20 nm. Other authors [33] find the PE lamellae from 7 to 20 nm. Due to experimental difficulties, measurements of lamella length are scarce. Authors have found only an estimate of the maximum length of PE lamellae in the range of 0.5–1 μm [33]. Believing that spherulite size is related to the lamellae length [34], spherulite dimension has been measured in the core of the injection molded plates of PP and PE. Spherulite pictures of 15 μm-thick microtomed slices were taken under a polarized light on an optical microscope Olympus BH-2 (Fig. 1). The PP spherulite diameter is about 40 μm and four times the PE spherulite diameter. Hence PP lamellae are assumed to be four times longer than the PE lamellae. As it will be discussed later, more than exact values of lamellae thickness or length, one of the key morphological parameters for micromechanical modeling is the ratio of length over thickness. Considering all the previous remarks, the ratio of length over thickness is higher for PP than for PE.

All materials parameters being determined, some micromechanical models aimed to estimate the elastic behavior of the homogeneous medium equivalent to a given heterogeneous material, are now presented.

2.2. Basic constitutive relations

Considering a heterogeneous microstructure with known micro-constituents properties, micromechanical modeling is aiming at establishing the behavior law of the equivalent homogeneous medium. When elastic behavior is considered only, the constitutive equations for the equivalent homogeneous medium may be written in terms of:

$$\boldsymbol{\Sigma} = \mathbf{C} : \mathbf{E} \tag{6}$$

where $\boldsymbol{\Sigma}$ and $\mathbf{E}$ denote the macro stress and macro strain tensor, respectively, $\mathbf{C}$ is the stiffness tensor of the semi-crystalline polymer.

Introducing the representative volume element V of the local properties, which contains a large number of micro-elements but has small dimensions in regard to the structure dimensions, $\boldsymbol{\Sigma}$ and $\mathbf{E}$ may be given in terms of the volume average stress and strain tensors:

$$\begin{aligned} \boldsymbol{\Sigma} &= <\boldsymbol{\sigma}>_V = \frac{1}{V}\int_V \boldsymbol{\sigma}(\mathbf{x})\mathrm{d}V \\ \mathbf{E} &= <\boldsymbol{\epsilon}>_V = \frac{1}{V}\int_V \boldsymbol{\epsilon}(\mathbf{x})\mathrm{d}V \end{aligned} \tag{7}$$

$\boldsymbol{\sigma}$ and $\boldsymbol{\epsilon}$ being the microscopic stress and microscopic strain tensors, respectively.

Due to Hill [35], strains (resp. stresses) in the heterogeneities are related to the macroscopic strains (resp. stresses) by the concentration-strain (resp. stress) tensor:

$$\boldsymbol{\epsilon}^{\mathrm{c}}(x) = \mathbf{A} : \mathbf{E} \qquad \boldsymbol{\sigma}^{\mathrm{c}}(x) = \mathbf{B} : \boldsymbol{\Sigma} \tag{8}$$

Hence a relation between $\boldsymbol{\Sigma}$ and $\mathbf{E}$ might be given in terms of:

$$\boldsymbol{\Sigma} = \frac{1}{V}\left(\int_{V^{\mathrm{c}}} \mathbf{C}^{\mathrm{c}} : \boldsymbol{\epsilon}^{\mathrm{c}}(x)\mathrm{d}V + \int_{V^{\mathrm{am}}} \mathbf{C}^{\mathrm{am}} : \boldsymbol{\epsilon}^{\mathrm{am}}(x)\mathrm{d}V\right) \tag{9}$$

where am stands for the amorphous phase and c for the crystalline phase. Finally $\mathbf{C}$ is simply defined by the relation:

$$\mathbf{C} = \mathbf{C}^{\mathrm{am}} + f^{\mathrm{c}}(\mathbf{C}^{\mathrm{c}} - \mathbf{C}^{\mathrm{am}}) : \mathbf{A} \tag{10}$$

where f^{c} is the volume fraction of the crystalline phase. The

assessment of the concentration-strain tensor **A** depends on the micromechanical model.

The isotropic spherulitic structure is very complex and taking into account this structure precisely seems incompatible with classical micromechanics model. Therefore two idealized representations of the materials have been chosen. On one hand the crystal lamellae are dispersed randomly in an amorphous matrix, on the other hand the material is made of an aggregate of composite inclusions, each inclusion consisting on a crystal lamella and an amorphous layer with a perfect interface. Both representations are now detailed.

2.3. Randomly distributed crystallites embedded in an amorphous matrix

In this representation, the crystalline phase is considered as a reinforcing phase embedded in an amorphous matrix. Crystal lamellae are approximated by ellipsoidal inclusions where direction 1 is the lamellae growth direction and direction 3 goes along the chain axis (Fig. 2).

To approximate the macroscopic tensor **C** representative of the elastic behavior of the equivalent homogeneous medium, some well known micromechanics models, which have been largely used for composite materials, are introduced.

The simplest models are the Voigt and Reuss bounds [36], which correspond to a homogeneous deformation and homogeneous stress in the material, respectively. Because of the high contrast between amorphous and crystalline phase moduli, both assumptions will give a result too far from the experiments. In another model due to Mori and Tanaka [37], the inclusions undergo the influence of other inclusions as equal as the average field in the matrix. This theory applies for volume fractions up to 30% only. Crystalline phase volume fractions encountered in our materials is out of the model validity range. In the self-consistent model, the material surrounding the inclusion is the equivalent homogeneous medium. This model is better suited for polycrystals or inclusion aggregates than the matrix/inclusion morphology [38].

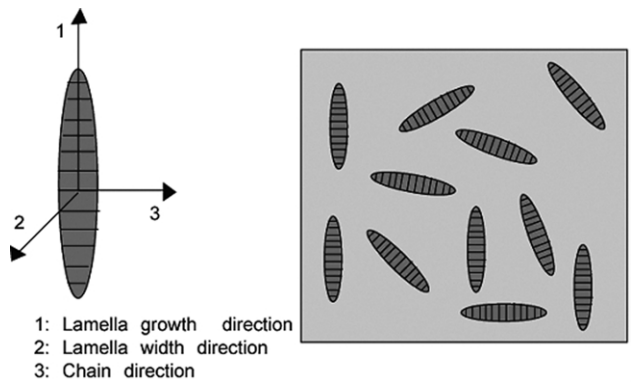

Fig. 2. Schematic illustration of crystal lamellae randomly distributed in the amorphous matrix. Direction 3 goes along the chain direction and direction 1 is the lamella growth direction.

Finally, the differential scheme is well designed when the volume fraction of the reinforcing phase is high [36]. The reinforcing phase is introduced by infinitesimally small increments using the dilute-distribution assumption. At the first increment the matrix surrounding the inclusion is the amorphous phase, at the following increments, the matrix surrounding the inclusion is characterized by a uniform elasticity, which has been calculated at the previous increment.

At each step $n+1$, the equivalent homogeneous medium stiffness tensor, $\mathbf{C}_{n+1}$, is evaluated from the following equations:

$$\mathbf{A}_n = \mathbf{I} + \mathbf{S}_n^{\mathrm{esh}}\,\mathbf{C}_n^{-1}(\mathbf{C}^{\mathrm{c}} - \mathbf{C}_n) \tag{11}$$

$$\mathbf{C}_{n+1} = \mathbf{C}_n + \delta f(\mathbf{C}^{\mathrm{c}} - \mathbf{C}_n) : \mathbf{A}_n$$

where **I** is fourth-order unity tensor, δf is the increment of crystal added at step $n+1$ and $\mathbf{S}_n^{\mathrm{esh}}$ is the Eshelby tensor [39] which depends on the inclusion ellipsoidal shape and on the elastic behavior of the surrounding material $\mathbf{C}_n$. This model will be used to estimate the stiffness tensor **C** for PP and various PE (low to HDPE). It will be also compared with another approach, which is very different from the matrix/inclusion model and developed specifically for semi-crystalline polymers by Lee et al. [18]. In this approach the material consists in an aggregate of composite layers as it is described in the following section.

2.4. Inclusion aggregate

The isotropic semi-crystalline polymer is represented by an aggregate of layered two-phase composite inclusions which are randomly oriented (Fig. 3). The angle between the chain axis direction c and the lamella normal n depends on the semi-crystalline polymer considered. As an example, the PE lamellae exhibit a tilt angle varying from 19° to 40° [40], whereas PP shows no tilt.

In this representation, both lamellae length and width are assumed to be very large in regards to the thickness, hence stresses and deformations within each phase may be considered as homogeneous. The composite inclusion stiffness tensor $\mathbf{C}^I(\boldsymbol{\sigma}^I = \mathbf{C}^I\boldsymbol{\epsilon}^I)$ is obtained by writing the interface compatibility and equilibrium [18]:

$$\epsilon^c_{\alpha\beta} = \epsilon^a_{\alpha\beta} = \epsilon^I_{\alpha\beta} \qquad (\alpha,\beta) \in \{1,2\}\times\{1,2\} \tag{12}$$

$$\sigma^c_{i3} = \sigma^a_{i3} = \sigma^{\mathrm{I}}_{i3},\ i \in \{1,2,3\} \tag{13}$$

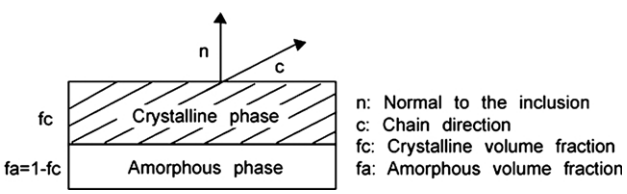

Fig. 3. Inclusion representation from Lee et al. [18].

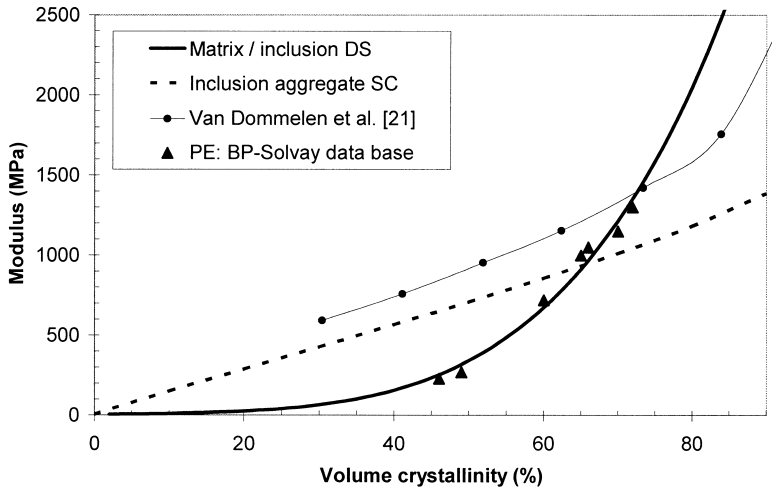

Fig. 4. Prediction of macroscopic PE Young's modulus versus volume crystallinity for ellipsoidal shape ratios $a_1/a_3 = 18$ and $a_2/a_3 = 5$.

and the mixture rule:

$$\mathbf{X}^{\mathrm{I}} = f_a \mathbf{X}^a + f_c \mathbf{X}^c \text{ for } \mathbf{X} = \boldsymbol{\sigma} \text{ or } \mathbf{X} = \boldsymbol{\epsilon} \tag{14}$$

Adopting the Voigt's notation, $\mathbf{C}^I$ is given in terms of the relation:

$$\sigma_K^I = \sum_{J=1,2,6} f_a (C_{KJ}^a - C_{KJ}^c)\epsilon_J^I + \sum_{J=3,4,5} f_a (C_{KJ}^a - C_{KJ}^c)\epsilon_J^a + \sum_{J=1}^{6} C_{KJ}^c \epsilon_J^I \tag{15}$$

where ϵ_J^a is given in terms of $\mathbf{C}^a, \mathbf{C}^c, f_a$ and $\boldsymbol{\epsilon}^I$ when using Eq. (13).

Once the inclusion behavior is known, a micromechanical model is applied to work out the isotropic behavior of the aggregate of randomly oriented inclusions. At this step, Nicolov et al. [41] have chosen a Sachs-type model while van Dommelen et al. [21] have used a hybrid model. Both models do not take into account any morphological parameters except for the tilt of the chain into the lamella. Knowing that the elastic behavior of respective phases and the crystallinity fraction cannot explain the lower modulus of HDPE compared to the PP modulus, can these models be relevant for both, PP and HDPE, polymers? Here, to account for morphological parameters, the self-consistent approach has been used since this model is appropriate for aggregate schematization. The homogeneous equivalent medium stiffness tensor $\mathbf{C}$ is then defined by the implicit relation:

$$\mathbf{C} = \mathbf{C} + f^c(\mathbf{C}^c - \mathbf{C}) : \mathbf{A}(\mathbf{C}) \tag{16}$$

$$\mathbf{A}(\mathbf{C}) = \mathbf{I} + \mathbf{S}^{\mathrm{esh}} \mathbf{C}^{-1} (\mathbf{C}^c - \mathbf{C})$$

and is evaluated with an iterative scheme, where the initial tensor $\mathbf{C}^0$ consists on the Voigt approximation stiffness tensor. The convergence conditions are written in terms of:

$$\sum_{K,L} |\mathbf{C}_{KL}^{n+1} - \mathbf{C}_{KL}^{n}| \leq \delta \tag{17}$$

and

$$\sum_{K,L} \left| \left(\frac{1}{m} \sum_{i=1}^{m} \mathbf{A}_{KL}^i \right) - \mathbf{I}_{KL} \right| \leq \delta \tag{18}$$

where m is the number of inclusions considered, $\mathbf{A}^i$ is the tensor of localization for inclusion i and $\mathbf{I}$ is the forth-order tensor.

This self-consistent scheme inclusion aggregate model is investigated in the case of PP and PE. In the next section, the inclusion aggregate model is compared to the differential scheme matrix/inclusion model for both materials.

3. Results and discussion

In this section, macroscopic elastic constants are calculated using the self-consistent composite inclusion aggregate model and the differential scheme matrix/inclusion model. The predicted results are compared to experimental data for PP and PE.

The number of randomly oriented inclusions within the matrix or within the aggregate should be sufficiently large in order to ensure isotropy; meanwhile, time of calculations should be reduced as much as possible. Here 200 orientations have been a good compromise to reach isotropy within an error of 5% in a limited time. For the differential scheme, the final homogeneous modulus depends on the prescribed increment of crystal volume fraction. In order to get a fair value of the homogeneous modulus, the increment must be taken sufficiently small; here a 2% increment is prescribed.

Considering for the PE lamellae, an average length from 0.5 to 1 μm as proposed by Michler and Godehardt [33], an average thickness of 20 nm [32] and a reasonably estimated width about 10 times the thickness, the calculated modulus overestimates largely the material modulus. As it has been discussed in Section 2, lamella shape ratios have not been

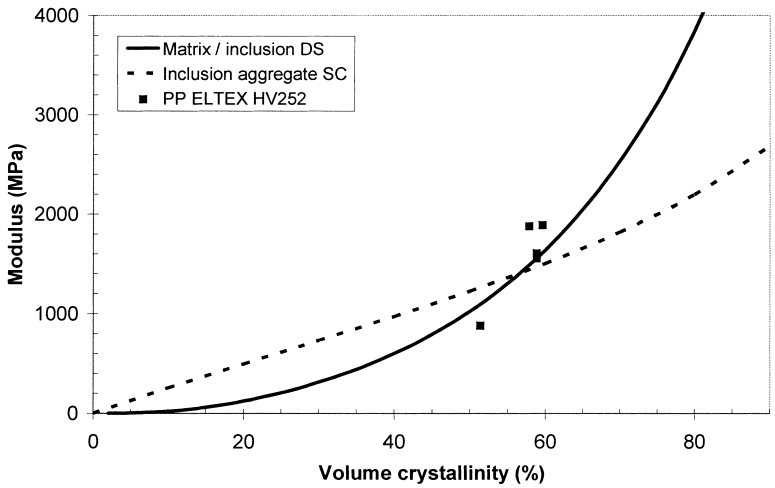

Fig. 5. Prediction of macroscopic PP Young's modulus versus volume crystallinity for ellipsoidal shape ratios $a_1/a_3 = 50$ and $a_2/a_3 = 5$.

defined precisely by experiments. Therefore values of the inclusion ellipsoidal shape ratios have been estimated for each material in order to reach an acceptable value for the Young's modulus. Denoting a_1, a_2 and a_3 the length, width and thickness of the lamella, two aspect ratios only are required to define the inclusion ellipsoidal shape. The shape parameters may be a_1/a_3 and a_2/a_3 for example. Fig. 4 presents the predicted macroscopic elastic modulus for PE as a function of the volume crystallinity. For the matrix/inclusion model, shape ratios equal to $a_1/a_3 = 18$ and $a_2/a_3 = 5$ while for the composite inclusion aggregate the shape ratios are equal to unity. In the case of the self-consistent composite inclusion aggregate, the condition of convergence in Eq. (18) cannot be reached for other shape ratios than unity. Therefore the self-consistent model defined in Eq. (16) is invalidated when the inclusion morphology is different from sphere [42].

The differential scheme matrix/inclusion model shows results in very good agreement with the experimental data. All calculations for both models were performed with a tilt angle of 40°. The composite inclusion aggregate model exhibits a curve shape that differs from experimental results and consequently experimental data cannot be fitted over the crystallinity range.

Results presented by van Dommelen et al. [21] are also plotted in Fig. 4. These results have been obtained with a composite inclusion aggregate hybrid model, which exhibits no morphology parameters except for the measured tilt of the chain in the lamella. Their results are far from the experimental data, especially for low crystallinities. Those authors attribute the deviation at low crystallinities to a change in the aspect ratio of lamellae that cannot be taken into account in their model. Introducing aspect ratios a_1/a_3 and a_2/a_3 equal to unity (a spherical inclusion, which minimizes the predicted moduli), the self consistent scheme composite inclusion aggregate model gives a predicted modulus over 670 MPa for a volume crystallinity of 45%, which still overestimates largely the experimental data: around 250 MPa.

We have also performed calculations for PP. Fig. 5 exhibits the estimated Young's modulus for inclusions shape ratios, $a_1/a_3 = 50$ and $a_2/a_3 = 5$ for the matrix/inclusion differential scheme model and the experimental data versus the crystal volume fraction. A good fit is

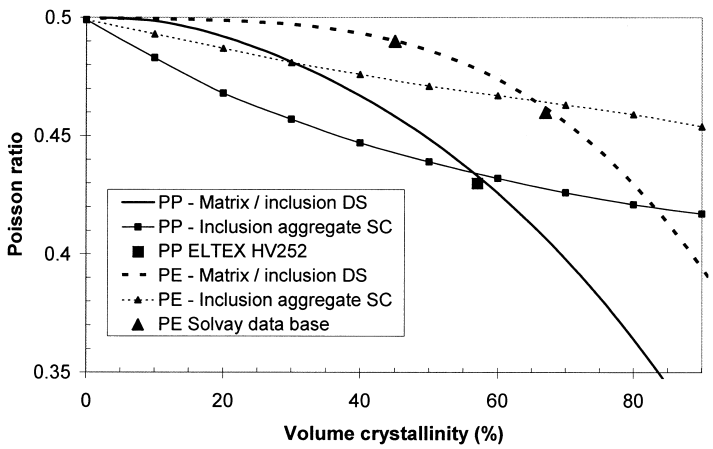

Fig. 6. Estimates of PE and PP Poisson's ratio versus volume crystallinity.

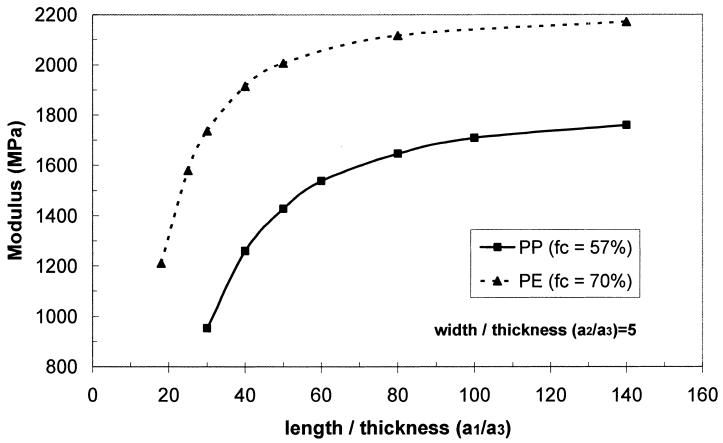

Fig. 7. Influence of the shape parameter length over thickness a_1/a_3 at a fixed width over thickness $a_2/a_3 = 5$ for the matrix/inclusion differential scheme model.

obtained with the differential scheme matrix/inclusion model. A good estimate at a fixed crystallinity of 57% is obtained with the composite inclusion aggregate model, but the shape of the curve is far from the expected one. In regards to the experimental data presented in the case of PE, one expects the same kind of curve shape for PP.

Poisson's ratio estimates have also been plotted versus crystallinity for both materials and both models in Fig. 6. As expected, the matrix/inclusion differential scheme model provides a good prediction of the Poisson's ratio, whereas the inclusion aggregate model underestimates this material parameter and overestimates the modulus.

For both materials, we have introduced values of inclusion aspect ratios that cannot be easily validated by physical measurements, but which have been physically motivated. First we have noted that the lamella thickness, which corresponds to the chain direction, must be small in regard with its length and width. Also the lamellae width must be small compared to the length. These remarks drive us to an oblate ellipsoidal shape for the inclusions. Secondly, the relative sizes of the spherulites on one part and of the lamella thickness on the other part for both PP and PE (see Section 2), suggest that aspect ratios are larger for PP than for PE. Hence, an explanation for the observed low macroscopic modulus of PE compared to PP one, despite a higher crystallinity and a higher modulus for each phase is given by the micromechanics model. The HDPE lower modulus compared to the PP modulus is due to smaller aspect ratios of the lamellae.

The influence of the aspect ratio parameters for the matrix/inclusion model has been quantified by considering the evolution of the homogeneous modulus at a fixed crystallinity with respect to the aspect ratio parameters. First, the parameter a_2/a_3 has been fixed equal to 5 while a_1/a_3 (length over thickness) goes from 18 to 140. Fig. 7 shows the homogeneous modulus variation versus a_1/a_3 for PP with a crystalline volume fraction equal to $f_c = 57\%$ and for HDPE with $f_c = 70\%$.

Other calculations with fixed length over thickness ratio, $a_2/a_3 = 18$ for HDPE and $a_1/a_3 = 50$ for PP, have been computed. The inclusion width may theoretically vary from the length to the thickness. Figs. 7 and 8 demonstrate the

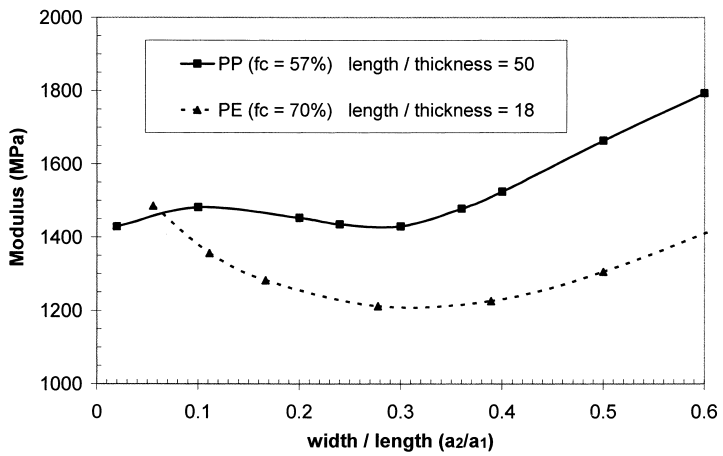

Fig. 8. Influence of the shape parameter width over length a_2/a_1, at a fixed length over thickness $a_1/a_3 = 20$ for the PE and $a_1/a_3 = 50$ for the PP, for the matrix/inclusion differential scheme model.

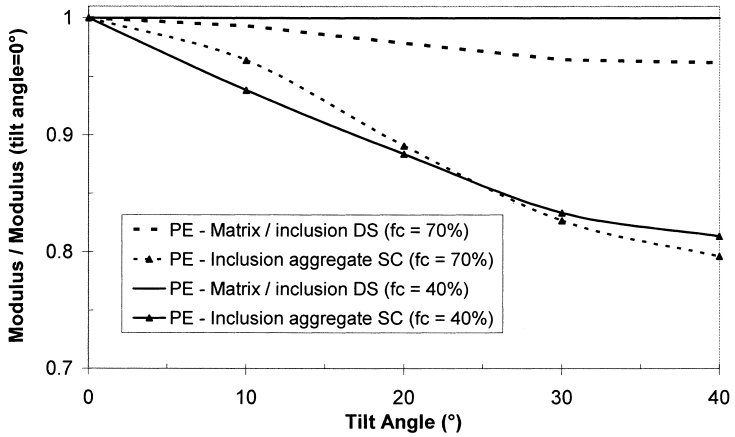

Fig. 9. Effect of PE lamellae tilt angle on the dimensionless modulus.

high influence of the inclusion aspect ratio on the final result. The modulus is shown to be more affected by the length over thickness parameter change, which may be explained by the large range of this parameter.

Finally, the influence of the tilt angle, which is defined as the angle between the chain axis direction c and the lamella normal n in the case of the composite inclusion aggregate model and between the chain axis direction c and the ellipsoidal thickness direction e_3 for the matrix/inclusion model, has been evaluated. When the angle goes from 0° to 40°, the modulus estimate varies within 5% for the matrix/inclusion model; hence the tilt angle has little influence on the final result. For the composite inclusion aggregate model, the modulus decreases when the tilt angle increases, the influence of the tilt angle is much stronger and goes up to 20%. These results are presented in Fig. 9 for the case of PE with 40% and 70% of crystallinity.

4. Conclusion

A micromechanical approach has been used for the prediction of isotropic elastic behavior of semi-crystalline polymers. Among several micromechanics models, two models have been especially investigated for their theoretical ability to represent semi-crystalline polymers: a differential scheme matrix/inclusion model and a self-consistent scheme composite inclusion aggregate. The material microstructure is represented by crystalline inclusions embedded into an amorphous matrix for the first model and by an aggregate of two-phase layered composite inclusions for the second one. The review of the elastic properties of each phase and of the respective crystalline volume fraction for two well known polymers (PP and PE), has proven the strong influence of some morphological parameters on the homogeneous modulus.

The present work has demonstrated the difficulties for the composite inclusion aggregate model to give satisfactory results concerning the elastic behavior of semi-crystalline polymers. This model overestimates largely the material modulus and underestimates logically the Poisson's ratio. Moreover it has no ability to capture a valuable physical morphological parameter.

On the contrary, the differential scheme matrix/inclusion model gave good estimates of the modulus and the Poisson's ratio for both isotropic materials. In this model, the inclusion aspect ratios are key morphological parameters, which explain a lower modulus for HDPE than for PP despite a higher rigidity for both phases and a higher crystallinity for HDPE. The model predicts an inclusion aspect ratio, length over thickness, larger for PP than for PE. This morphological difference is relevant with experimental measurements of a mean spherulite radius about four times larger for PP than for PE injection molded samples and of a lamella thickness around twice smaller for PP than for PE.

Finally, this work underlines the interest on developing measurements not only on the lamella thickness but also on the width and length of lamellae. The lamella thickness only, cannot be relevant for prediction of the material elastic constants.

References

[1] Lovinger A. J Polym Sci, Polym Phys Ed 1983;21:97.
[2] Ward IM. Structure and properties of oriented polymer. London: Chapman and Hall; 1997.
[3] Gorlier E, Haudin JM, Billon N. Polymer 2001;42:9541–9.
[4] Pople JA, Mitchell GR, Sutton SJ, Vaughan AS, Chai CK. Polymer 1999;40:2769–77.
[5] Ülçer Y, Camak M. Polymer 1997;38:2907–23.
[6] Mendoza R, Regnier R, Seiler W, Lebrun JL. Polymer 2003;44:3363–73.
[7] Trotignon JP, Verdu. J Appl Polym Sci 1990;39:1215–7.
[8] Philips R, Herbert G, News J, Wolkovics M. Polym Engng Sci 1994;34:1731–43.
[9] Chevalier L, Linhone C, Régnier G. Plast Rubber Comp 1999;28:393–400.
[10] Titomanlio G, Jansen KMB. Polym Engng Sci 1996;36:2041–9.
[11] Mac Leish TCB, Larson RG. J Rheol 1998;42:81–110.
[12] Doufas AK, Dairanieh IS, McHugh AJ. J Rheol 1999;43:85–109.

[13] Poitou A, Ammar A. C R Acad Sci (Paris) Serie II 2001;329:5–11.
[14] Tucker CL, Liang E. Comp Sci Technol 1999;59:655–71.
[15] Halpin JC, Kardos JL. J Appl Phys 1972;43:2235–41.
[16] Tsai SW, Halpin JC, Pagano NJ. Composite Materials Workshop (Technomic, Stamford, Conn., 1968).
[17] Phillips PJ, Patel J. Polym Engng Sci 1978;18:943–50.
[18] Lee BJ, Argon AS, Parks DM, Ahzi S, Bartczak Z. Polymer 1993;34: 3555–75.
[19] Dahoun A, Aboulfaraj M, G'Sell C, Molinari A, Canova GR. Polym Engng Sci 1995;35:317–30.
[20] Nikolov S, Doghri I. Polymer 2000;41:1883–91.
[21] van Dommelen JAW, Parks DM, Boyce MC, Brekelmans WAM, Baaijens FPT. J Mech Phys Solids 2003;51:519–41.
[22] Flory PJ. Principles of polymer chemistry. Ithaca, NY: Cornell University Press; 1953.
[23] Graessley WW, Edwards SF. Polymer 1981;22:1329–34.
[24] Wu S. J Polym Sci, Polym Phys Ed 1989;27:723–41.
[25] Fetters LJ, Loshe DJ, Graessley WW. J Polym Sci, Polym Phys Ed 1999;37:1023–33.
[26] Van Krevelen DW. Properties of polymers, third completely revised edition. Amsterdam: Elsevier; 1990.
[27] Zoller P, Walsh D. Standard pressure-volume-temperature data for polymers. Technomic; Lancaster, USA 1995.
[28] Choy CL, Leung WP. J Polym Sci, Polym Phys Ed 1985;23:1759–80.
[29] Tashiro K, Kobayashi M, Tadokora H. Polymer 1996;37:1775–86.
[30] Tashiro K, Kobayashi M, Tadokora M. Polymer 1992;24:899–916.
[31] Sawatari C, Matsuo M. Macromolecules 1986;19:2653–5.
[32] Robelin-Souffaché E, Rault J. Macromolecules 1989;22:3581–99.
[33] Michler GH, Godehardt R. Cryst Res Technol 2000;35:863–75.
[34] Phillips PJ, Sien HP. Polym Engng Sci 1978;18:299–305.
[35] Hill R. J Mech Phys Solids 1963;11:357–72.
[36] Nemat-Nasser S, Hori M. Micromechanics: overall properties of heterogeneous materials, second revision edition. Elsevier, Amsterdam 1999.
[37] Mori T, Tanaka K. Acta Metallurgica 1973;21:571–4.
[38] Gilormini P, Brechet Y. Mod Simul Mater Sci Engng 1999;17: 805–16.
[39] Mura T. Micromechanics of defects in solids, second revised edition. Dordecht: Kluwer; 1987.
[40] Hoffman JD, Miller RL. Polymer 1997;38:3151–212.
[41] Nikolov S, Doghri I, Pierard O, Zealouk L, Goldberg A. J Mech Phys Solids 2002;50:2275–302.
[42] Walpole LJ. J Mech Phys Solids 1969;17:235–51.